Environmental Pollution 196 (2015) 497–510

Contents lists available at ScienceDirect

Environmental Pollution

journal homepage: www.elsevier.com/locate/envpol

Atmospheric deposition of nitrogen, sulfur and base cations in jack pine stands in the Athabasca Oil Sands Region, Alberta, Canada

M.E. Fenn*, A. Bytnerowicz, S.L. Schilling, C.S. Ross

USDA Forest Service, Pacific Southwest Research Station, 4955 Canyon Crest Drive, Riverside, CA 92507, USA

ARTICLE INFO

Article history:
Received 15 January 2014
Received in revised form
6 August 2014
Accepted 25 August 2014
Available online 16 September 2014

Keywords:
Boreal forests
Fossil fuel extraction
Fire emissions
Atmospheric deposition gradient
Ion exchange resin samplers

ABSTRACT

Atmospheric deposition in the Athabasca Oil Sands Region decreased exponentially with distance from the industrial center. Throughfall deposition (kg ha^{-1} yr^{-1}) of NH_4–N (.8–14.7) was double that of NO_3–N (.3–6.7), while SO_4–S ranged from 2.5 to 23.7. Gaseous pollutants (NO_2, HNO_3, NH_3, SO_2) are important drivers of atmospheric deposition but weak correlations between gaseous pollutants and deposition suggest that particulate deposition is also important. The deposition (eq ha^{-1}) of base cations (Ca + Mg + Na) across the sampling network was highly similar to N + S deposition, suggesting that acidic deposition is neutralized by base cation deposition and that eutrophication impacts from excess N may be of greater concern than acidification. Emissions from a large forest fire in summer 2011 were most prominently reflected in increased concentrations of HNO_3 and throughfall deposition of SO_4–S at some sites. Deposition of NO_3–N also increased as did NH_4–N deposition to a lesser degree.

Published by Elsevier Ltd.

1. Introduction

The oil reserves within the Athabasca Oil Sands Region (AOSR) in northern Alberta, Canada (Fig. 1) constitute the third largest in the world, trailing only those in Venezuela and Saudi Arabia (United States Energy Information Administration; http://www.eia.gov). Production of crude bitumen from the oil sands reached 9.6 Gj d^{-1} in 2010 or about 2% of world oil production (Englander et al., 2013). The tar sands are mined by open pit mining as well as by in-situ methods (e.g., steam assisted gravity drainage). The bitumen is extracted from the oil sands and upgraded to synthetic crude oil. Industrial activities associated with mining and processing results in significant atmospheric emissions of nitrogen, sulfur and other pollutants with potential to affect the surrounding ecosystems (Percy et al., 2012).

Access to the boreal forests and wetlands surrounding the industrial zone of the AOSR is primarily by helicopter; thus passive air pollution sampling methods that do not need electric power and that require low-frequency site visits are desirable for monitoring air quality and deposition inputs across these remote areas (Bytnerowicz et al., 2010a,b; Fenn and Ross, 2010; Fenn et al., 2009; Proemse et al., 2012). A passive sampling method for measuring bulk deposition in forest clearings or throughfall deposition based on the deployment of ion exchange resin (IER) columns connected to a sampler funnel has been successively used in many field studies (Fenn and Poth, 2004; Fenn et al., 2008; Root et al., 2013), including the AOSR (Fenn and Ross, 2010; Fenn et al., 2013; Laxton et al., 2012; Proemse et al., 2012; Wieder et al., 2010). The IER sampling method is very useful for deposition monitoring in remote regions because of the infrequent sampling requirements. However, it is also advantageous in local studies because of the greatly reduced number of analytical samples, even though the procedures of column extraction and chemical analysis are more rigorous than required for simple aqueous samples.

In this study atmospheric deposition of nitrogen (N) and sulfur (S) to the boreal forests surrounding the industrial zone in the AOSR was monitored for four years across a network of jack pine (*Pinus banksiana* Lamb.) study sites. Measurement of nutrient deposition in throughfall is a widely used method for estimating atmospheric deposition inputs to forest ecosystems (Bleeker et al., 2003; Parker, 1983; Thimonier, 1998). In addition to wet deposition of pollutants from the atmosphere during precipitation events, large amounts of pollutants are dry-deposited to surfaces such as tree canopies. A large fraction of these dry-deposited pollutants are periodically washed off by precipitation. This hydrologic dissolution of accumulated pollutant deposition on the forest canopy, in addition to leaching of ions from vegetative tissue, is referred to as throughfall. Thus, throughfall deposition may be defined as the hydrologic flux to the forest floor of ions and other compounds contained within the throughfall solution (Parker, 1983).

* Corresponding author.
E-mail address: mfenn@fs.fed.us (M.E. Fenn).

http://dx.doi.org/10.1016/j.envpol.2014.08.023
0269-7491/Published by Elsevier Ltd.

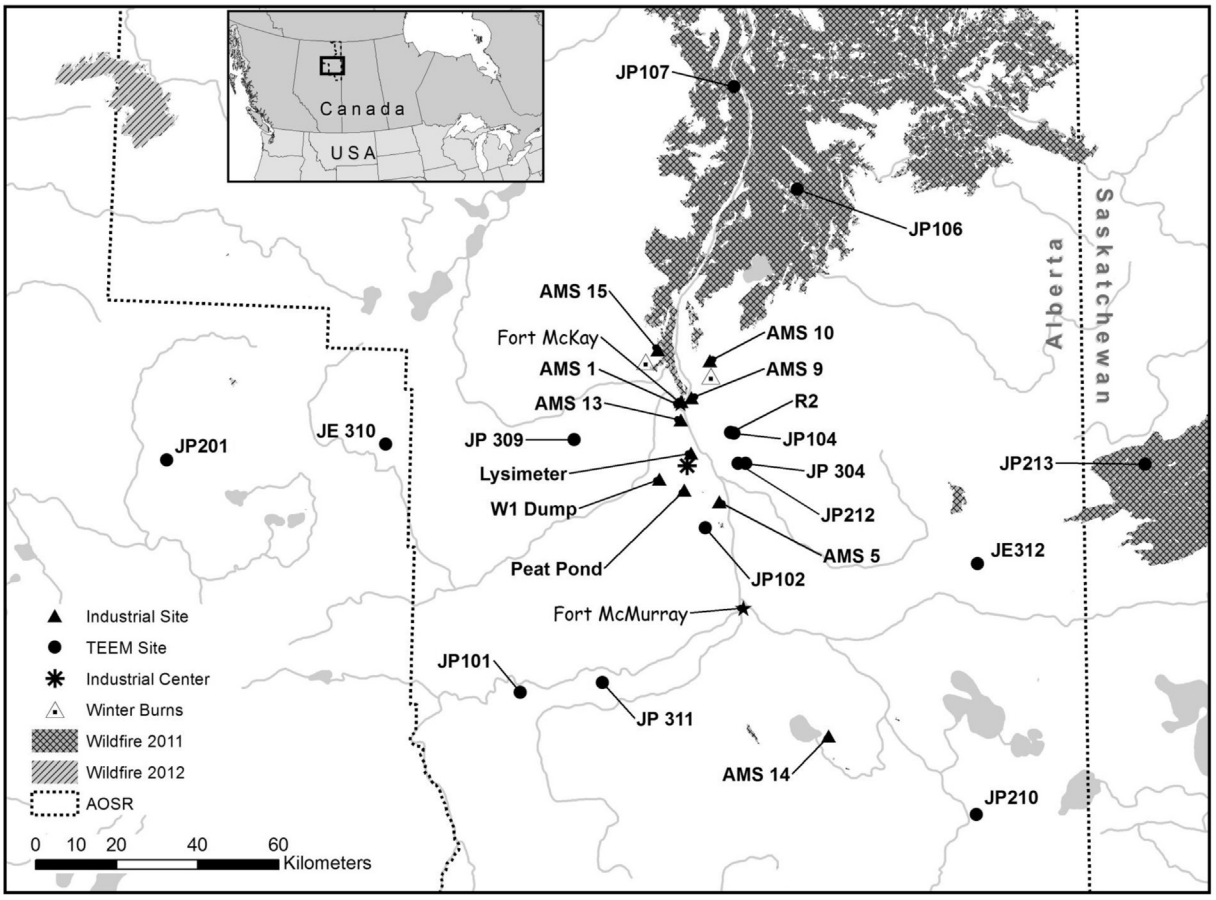

Fig. 1. Location of the Athabasca Oil Sands Region (AOSR) in Alberta, Canada and of the deposition monitoring sites reported on in this study. TEEM (Terrestrial Environmental Effects Monitoring) sites are jack pine (JP) forest health plots and the industrial sites show the location of AMS (air monitoring stations) located within or adjacent to the industrial zone. The towns of Fort McKay and Fort McMurray are indicated by star symbols.

The objective of this study is to measure atmospheric deposition levels and characterize spatial gradients and seasonal trends of deposition to the forest surrounding and downwind of the major industrial zone in the AOSR. A major question to be addressed by this research was to evaluate the spatial extent of the zone of influence resulting from atmospheric emissions of N and S from the industrial processes within the AOSR. The relationship between atmospheric concentrations of gaseous N and S pollutants and deposition levels across the network was also evaluated as a preliminary assessment of the dominant drivers of dry deposition in the AOSR. Base cation deposition was also measured for one year, allowing a comparison of atmospheric inputs to the forest of acidifying N and S deposition versus base cation deposition. Because of a large forest fire in the AOSR in summer 2011 and two controlled wood burning activities in early winter 2012, the effects of fire on N and S gaseous pollutants and atmospheric deposition were also evaluated.

2. Materials and methods

2.1. Study sites

Beginning in the late 1990s the Terrestrial Environmental Effects Monitoring (TEEM) program, operated by the Wood Buffalo Environmental Association (WBEA), established a network of long-term monitoring sites in jack pine stands within the Athabasca Oil Sands Region (AOSR). These sites were chosen to be "ecologically analogous" (Laxton et al., 2010) by meeting a suite of criteria including extensive landscape, vegetation, soil and other geographical characteristics, such as distance from roads and other development factors. In this study bulk deposition of nitrogen and sulfur in precipitation and throughfall was measured at a subset of the TEEM jack pine plots from May 2008 to May 2012 (Table 1). Deposition measurements were also taken at several industrial monitoring sites (Table 1) located closer to the emissions source area. Sites selected for deposition measurements were chosen to provide an estimate of spatial patterns in atmospheric deposition. As the larger jack pine network evolved and expanded, the sites selected for deposition monitoring also changed; thus discontinuity in the sites selected for deposition measurements can be seen in Table 1.

The AOSR is predominantly located in the Boreal Plains ecozone. The region experiences a continental climate with warm summers and cold winters. The terrestrial landscape is composed largely of muskeg peatlands where black spruce (*Picea mariana* (Mill.) B.S.P.) is common, but mineral soil uplands commonly feature jack pine, with balsam fir (*Abies balsamea* (L.) Mill.) and trembling aspen (*Populus tremuloides* Michx.) also present. Annual precipitation in Fort McMurray (airport station) is 455.5 mm and the mean annual temperature is .7 °C (average 1971–2000; Environment Canada, 2011). Lowest average monthly precipitation rates occur from December through March when the sum of monthly averages is 69.7 mm (years 1971–2000) and precipitation is highest in July when the average precipitation for the same time period was 81.3 mm. Precipitation at three locations within the AOSR during the summer and winter seasons during the four years of this study are shown in Fig. 2. One of the major stacks in the AOSR near Fort McMurray (57.048°N, 111.616°W) was used as a central marker point for the industrial emissions, as described by Proemse et al. (2012). Distances between the stack and the sampling sites vary between 3 and 129 km (Fig. 1).

2.2. Throughfall deposition measurements

Throughfall and bulk precipitation samples were collected with "passive" throughfall collectors based on a mixed bed (cation and anion resin) ion exchange resin (IER) column (Fenn and Poth, 2004; Fenn et al., 2009). The IER columns are filled with Amberlite™ IRN 150 Mixed Bed analytical grade ion exchange resin beads pre-rinsed with distilled deionized water. Precipitation or throughfall samples are collected by a polyethylene funnel or snow tube and channeled through the resin column, where ions are retained by the ion exchange resin. The major advantage of

Table 1
Industrial and Terrestrial Environmental Effects Monitoring (TEEM) sites at which atmospheric deposition data were collected. AMS sites are long-term Air Monitoring Stations and JP sites are jack pine forest health plots.

Site name	Type	Distance from the industrial center (km)	2004 Stocking Density, 2011 in parentheses (stems/ha)[a]	2004 Stand Age, 2011 in parentheses (yrs)[a]	Latitude	Longitude	IER season collection							
							S 08	W 08	S 09	W 09	S 10	W 10	S 11	W 11
Industrial sites														
AMS 1	Open	16			57.1895	−111.6405	✓	✓		✓	✓	✓	✓	✓
AMS 1	TF		na	na			✓	✓		✓	✓	✓	✓	✓
AMS 5	Open	12			56.9679	−111.4820	✓	✓		✓				
AMS 5	TF		na	na			✓	✓		✓				
AMS 9	Open	17			57.1982	−111.5996	✓	✓		✓				
AMS 9	TF		na	na			✓	✓		✓				
AMS 10	Open	27			57.2810	−111.5257	✓	✓						
AMS 10	TF		na	na			✓	✓						
AMS 13	Open	13			57.1491	−111.6426	✓	✓	✓	✓				
AMS 13	TF		na	na			✓	✓	✓	✓				
AMS 14	Open	75			56.4493	−111.0372	✓	✓		✓	✓	✓	✓	✓
AMS 14	TF		na	na			✓	✓	✓	✓	✓	✓	✓	
AMS 15	Open	29			57.3037	−111.7396	✓	✓	✓	✓				
AMS 15	TF		na	na			✓	✓	✓	✓				
Lysimeter	Open	3			57.0753	−111.5984	✓	✓	✓	✓	✓	✓		✓
Lysimeter	TF		na	na			✓	✓	✓	✓	✓	✓		✓
Peat Pond	Open	6			56.9932	−111.6248	✓	✓	✓	✓	✓	✓		
Peat Pond	TF		na	na										
W1 Dump	Open	8			57.0170	−111.7271	✓	✓	✓	✓	✓	✓		
W1 Dump	TF		na	na										
TEEM sites														
JP 101	Open	70			56.5399	−112.2767					✓	✓	✓	✓
JP 101	TF		700 (600)	48 (na)							✓	✓	✓	✓
JP 102	Open	16			56.9102	−111.5381	✓	✓	✓	✓	✓	✓	✓	✓
JP 102	TF		700 (675)	52 (68)			✓	✓	✓	✓	✓	✓	✓	✓
JP 104	Open	14			57.1208	−111.4242	✓	✓	✓	✓	✓[b]	✓	✓	✓
JP 104	TF		800 (775)	65 (na)			✓	✓	✓	✓	✓	✓	✓	✓
R2	Open	14			57.1216	−111.4378								
R2	TF		800 (775)	65 (na)			✓	✓	✓	✓	✓	✓	✓	✓
JP 106	Open	73			57.6620	−111.1684					✓	✓	✓	✓
JP 106	TF		2675 (1150)	68 (82)							✓	✓	✓	✓
JP 107	Open	94			57.8895	−111.4336	✓	✓	✓	✓	✓	✓		
JP 107	TF		1350 (na)	57 (na[c])			✓	✓	✓	✓	✓	✓		
JP 201	Open	129			57.0320	−113.7340					✓	✓	✓	✓
JP 201	TF		2125 (1325)	55 (na)							✓	✓	✓	✓
JP 210	Open	112			56.2736	−110.4484					✓	✓	✓	✓
JP 210	TF		1600 (1075)	69 (83)							✓	✓	✓	✓
JP 212	Open	13			57.0539	−111.4072	✓	✓	✓	✓	✓	✓	✓	✓
JP 212	TF		1900 (1525)	55 (na)			✓	✓	✓	✓	✓	✓	✓	✓
JP 213	Open	113			57.0464	−109.7488	✓	✓	✓	✓	✓	✓	✓	✓
JP 213	TF		975 (750)	53 (70)			✓	✓	✓	✓	✓	✓	✓	✓
JP 304	TF	15	na (850)	na (71)	57.0536	−111.3761							✓	✓
JP 309	TF	29	na	na	57.1020	−112.0754							✓	✓
JE 310	Open	75	na (1400)	na (71)	57.0833	−112.8447							✓	
JE 311	Open	57			56.5645	−111.9471							✓	✓
JP 311	TF		na (525)	na (55)									✓	✓
JE 312	Open	76			56.8300	−110.4347							✓	✓
JP 312	TF		na (675)	na (88)									✓	

[a] 2004 stocking density and stand age data from Jones and Associates Ltd., 2007. 2011 data are unpublished data.
[b] At JP104 there was no change-out for the open site in October 2010, so these collectors provided annual deposition data for May 2010 to May 2011.
[c] At the JP107 site all the trees were dead in the 2011 survey because of the large wildfire that occurred in summer 2011.

the IER method is that sample collection continues in the field without the need for repeated field trips to collect liquid samples or the need for repeated sample analyses from each collector. This is highly advantageous in the Athabasca study region where many sites are only accessible by helicopter at great logistical effort and expense.

The inner diameter of the funnels used for the IER collectors is 21.1 cm and the funnel collectors have a vertical wall 10 cm in height. Snow tubes 50 cm in height with an inner diameter of 20.2 cm were inserted into the funnels to allow for snow collection. Bird rings modeled after the design of Asman et al. (1982) made from "tomato cages" larger in diameter than the snow tubes were installed above the collectors and Teflon-coated fishing line was strung across the bird rings to discourage birds from perching on the collectors. The IER columns for the summer exposures were installed in May and changed out in October. Winter exposures were from October to May. Preliminary tests in forest clearings in the AOSR comparing snow collection efficiency of the snow tubes (320 cm^2) with snow buckets (465 cm^2) indicated that the snow buckets collected 32% more snow than the snow tubes (average of 2 sites). Differences between collection efficiencies of the snow tubes versus snow buckets was found to be much less under canopies, presumably because the canopies partially buffer the effects of wind on snow collection. Thus, it is assumed that winter deposition of snow is underestimated by the snow tube collectors, and by a greater proportion in open sites.

At each monitoring site four collectors were installed in an open area and eight under jack pine canopies. The open areas were commonly in a remnant burn site or in a bog. Deposition measured in open sites or forest clearings is conventionally referred to as bulk precipitation or bulk deposition; use of the term 'bulk' refers to the fact that the funnel collectors are continuously opened to the atmosphere resulting in accumulation of some dry-deposited material to the funnels, particularly during extended dry periods. However, atmospheric deposition collected is predominantly wet deposition sampled during precipitation events. Near each open site eight IER samplers are installed in jack pine canopies, by installing two collectors per tree on four trees. In the boreal forests of the AOSR experience has shown that black bears routinely disturb IER collectors, requiring that samplers be protected from bears. To prevent bear disturbance of the samplers, solar-powered electric fences were installed around the sampling areas in remote sites. Electric fences were

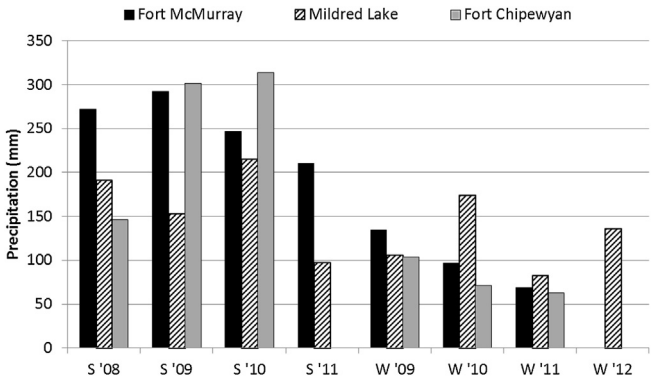

Fig. 2. Seasonal (summer and winter) sums of precipitation at three locations within the study region. The Mildred Lake site is 4 km east of the industrial center and Fort Chipewyan is 194 km north of the industrial center. Data are from the Climate office of the Canadian Government: http://climate.weatheroffice.gc.ca/climateData/canada_e.html. Data are the sums of daily total precipitation.

not used when sampling in bogs or at air monitoring stations close to areas of high human traffic or activity.

Twenty-five grams of the ion exchange resin beads were poured into PVC tubes (20 cm in length and 1.25 cm I.D.) as an aqueous slurry and then further rinsed with distilled water. After the field exposure periods the IER columns were extracted with 75 ml of 1*N* KI, followed by a second extraction with 75 ml of 1*N* KI. Nitrate and sulfate concentrations in the column extracts were analyzed by ion chromatography (Dionex DX-1600, Sunnyvale, CA) using a procedure modified from Simkin et al. (2004). Ammonium concentrations in the KI extracts were determined colorimetrically (Technicon TRAACS autoanalyser). Quality control measures included a blank IER tube that was capped and deployed with other tubes on-site for the same length of time, in addition to analysis of laboratory standards and of random duplicate samples. Phosphate concentrations in the IER column extracts were also measured using ion chromatography to aid in the detection of bird dropping contamination. Samples designated for base cation analysis received an additional extraction of 200 ml KCl. The KI and KCl extracts were proportionately combined and analyzed for Ca, Mg and Na by ICP-AES (inductively coupled plasma atomic emission spectroscopy) at the Maine Agricultural and Forestry Experiment Station analytical laboratory at the University of Maine in Orono. Atmospheric deposition fluxes were determined by extrapolating from the area of the collector opening and the amounts of inorganic N and S or base cations that were extracted from the IER columns (Fenn and Poth, 2004; Fenn et al., 2009).

Spatial patterns of deposition amounts with increasing distance from the industrial center of the oil sands were determined by plotting deposition fluxes versus distance and curve fitting this relationship. Deposition data from the AMS14 industrial site, located 74 km southeast of the industrial center, was excluded because of the confounding factor of local emissions sources of N, S and base cations from the mining operations in the area. The Regression Wizard in SigmaPlot version 11 (Systat Software Inc., San Jose, CA, USA) was used for curve fitting and statistical analysis of the relationship. The 2-parameter power equation ($y = ax^b$) was selected for curve fitting, with the constraint that $b < 0$. The dependent variable (y) is atmospheric deposition flux (kg ha^{-1}) and the independent variable (x) is distance from the industrial center based on the location of the major emissions stack mentioned above. The Regression Wizard uses an iterative process to find the best fit parameters (a, b). A report is created with the fitted parameters and an analysis of variance (ANOVA) of the regression including *P* values. Because of a lack of annual base cation deposition data for sites at mid-range distances from the industrial center (because of several changes between seasons in the sites used to monitor base cations), we used the distance/deposition regression relationship for annual DIN + S deposition to predict annual base cation deposition with distance from the industrial center. Previous tests using summer and winter seasonal data demonstrated that base cation and DIN + S distance/deposition relationships were virtually identical.

2.3. Passive monitoring of gaseous pollutants

Atmospheric concentrations of nitric acid vapor (HNO_3), ammonia (NH_3), nitrogen dioxide (NO_2) and sulfur dioxide (SO_2) were measured at the study sites using passive samplers. A major objective for measuring these pollutants was to determine their importance as drivers of atmospheric deposition of N and S in the AOSR. Nitrogen dioxide was measured with Maxxam NO_2 samplers (Tang et al., 1999), SO_2 with Maxxam SO_2 samplers (Tang et al., 1997), NH_3 with Ogawa NH_3 samplers (Roadman et al., 2003) and HNO_3 with the nylon filter method (Bytnerowicz et al., 2005). Nitric acid samplers based on nylon filters, such as those used in this study (Bytnerowicz et al., 2010a) accumulate both HNO_3 and HNO_2 (nitrous acid; Bytnerowicz et al., 2005), thus the HNO_3 data reported herein includes a small proportion of co-measured HNO_2).

Gaseous concentration data from the passive samplers are only presented for sites co-located with the IER collectors, although when evaluating effects of fire emissions on air quality, data from the larger passive sampler monitoring network were included in the analysis. The samplers for HNO_3 and NH_3 were changed every month between May 1st through October 31st and every two months between November 1st and April 30th. The NO_2 and SO_2 samplers were changed monthly at the AMS1 and AMS14 monitoring stations and 9 times per year at the remote sampling sites (Hsu, 2012). Thus the passive samplers provide time-averaged concentration values for the exposure period.

Three replicate samplers were used at each site for HNO_3. Two replicate samplers were deployed at each site for NO_2 and SO_2. In the case of NH_3, one sampler containing two replicate filters per sampler was deployed at each site. At the remote sites samplers were located above the forest canopy at a height of about 10 m above ground level on towers. At all other sites the passive samplers were placed on wooden posts about 2 m above ground level. Further details and a description of laboratory analyses of the passive samplers are described in Bytnerowicz et al. (2010a) and Hsu (2012). Passive sampler data for all the gaseous pollutants mentioned above were collected during the four years of the study (summer 2008 to winter 2011/2012) at seven sites for NO_2 and SO_2 and 16 sites for NH_3 and HNO_3 (Bytnerowicz et al., 2010a).

The relationship between atmospheric concentrations of gaseous N and S pollutants and deposition levels across the network were determined by linear regression of the average atmospheric concentrations of HNO_3, NO_2, NH_3, and SO_2 versus deposition fluxes of NO_3–N, NH_4–N, dissolved inorganic N (DIN; NO_3–N + NH_4–N), or SO_4–S. Data were combined from the four years of the study (May 2008 to May 2012).

3. Results

3.1. Spatial and seasonal patterns of deposition for N, S and base cations

Annual deposition of NH_4–N in throughfall across the monitoring sites in the AOSR ranged from .8 to 14.7 kg ha^{-1} compared to a range of .3–6.7 kg ha^{-1} for throughfall NO_3–N. Deposition of SO_4–S in throughfall ranged from 2.5 to 23.7 kg ha^{-1} yr^{-1}. Deposition of NH_4–N, NO_3–N and SO_4–S in bulk precipitation across the network ranged from .8 to 2.8, .4–1.6 and 1.0–6.8 kg ha^{-1} yr^{-1}, respectively (Table 2). At a distance of 20 km from the industrial center, bulk deposition of NH_4–N, NO_3–N, DIN, SO_4–S and base cations were all similarly enriched by a factor of 2–4 compared to background (Table 2). Bulk deposition for all these ions except base cations at 3 km from the industrial center were enriched 4–7 fold compared to background sites; while base cations were enriched 11-fold. Throughfall deposition of NH_4–N, NO_3–N and DIN were 18–25 times greater at 3 km from the industrial center compared to background, while the enrichment ratio for SO_4–S and base cations in throughfall was 10 and 13, respectively (Table 2).

Atmospheric deposition of N, S and base cations all showed a similar pattern of rapidly decreasing values with distance from the industrial center, particularly in throughfall. Atmospheric deposition declines approximately with the inverse square root of the distance from the industrial center (Fig. 3). Throughfall deposition of SO_4–S and DIN decreased from maximum values of 24 and 22 kg ha^{-1} yr^{-1} at 3 km from the emissions sources to predicted values of 11 and 3 kg ha^{-1} yr^{-1} at 20 km from the industrial center – a decrease of 56% and 88%, respectively (Table 2). Spatial trends in throughfall DIN deposition became relatively flat at around 24 km from the industrial center (throughfall deposition of 2.1 kg ha^{-1} yr^{-1}) with deposition more than 90% less than in the industrial center. DIN in throughfall was already reduced by 75% at only 10.5 km from the industrial center (Fig. 3). In contrast, moderately elevated fluxes of S in throughfall extended further away from the emissions sources than N deposition, with S deposition in throughfall reduced by 75% at 53 km from the industrial center and by 80% and 90% at predicted distances of 84 and 353 km (Fig. 3).

Deposition of NH_4–N and NO_3–N in throughfall decreased more precipitously with distance from the industrial center than is the case for bulk deposition in open areas. Deposition of NH_4–N declined by

Table 2
Annual and seasonal deposition fluxes in the AOSR at the most and least exposed sites and at 20 km from the industrial zone and deposition ratios compared to background at 20 km and 3 km from the industrial center. Values in parentheses are standard errors except for predicted values at 20 km which are 95% confidence intervals for the regression.

Deposition level[a]	NH_4–N (kg ha^{-1})	NO_3–N (kg ha^{-1})	DIN (kg ha^{-1})	SO_4–S (kg ha^{-1})	Base cations[b] (eq ha^{-1})	DIN + S (eq ha^{-1})
Summer—open sites						
Maximum (at 3 km)	1.8 (.16)	.99 (.23)	2.8 (.37)	3.8 (.53)	693	441 (57)
At 20 km	1.39 (±.44)	.60 (±.13)	2.0 (±.53)	2.4 (±.57)	301	301 (±75)
Background (113–129 km)	.6 (.11)	.25 (.05)	.85 (.15)	.72 (.13)	93	106 (19)
Percent decrease at 20 km	24	39	30	36	57	32
Ratio 20 km:Background	2.3	2.4	2.4	3.4	3.2	2.8
Ratio 3 km:Background	3.1	4.0	3.3	5.3	7.5	4.2
Winter—open sites						
Maximum (at 3 km)	.86 (.12)	.66 (.07)	1.5 (.10)	3.2 (.43)	530	308 (28)
At 20 km	.41 (±.09)	.42 (±.06)	.84 (±.13)	1.9 (±.51)	180	180 (±40)
Background (113–129 km)	.20 (.04)	.17 (.03)	.37 (.07)	.29 (.04)	16	45 (7)
Percent decrease at 20 km	52	36	45	41	66	42
Ratio 20 km:Background	2.0	2.5	2.3	6.5	11.0	4.0
Ratio 3 km:Background	4.2	4.0	4.1	11.0	32.5	6.9
Annual—open sites						
Maximum (at 3 km)	2.8 (.11)	1.6 (.3)	4.4 (.28)	6.8 (.94)	1223	741 (73)
At 20 km	1.8 (±.53)	1.0 (±.17)	2.8 (±.65)	4.1 (±.85)	468	468 (±98)
Background (113–129 km)	.8 (.08)	.4 (.04)	1.2 (.11)	1.0 (.1)	109	150 (13)
Percent decrease at 20 km	35	39	36	40	62	37
Ratio 20 km:Background	2.3	2.4	2.3	4.1	4.3	3.1
Ratio 3 km:Background	3.5	4.0	3.6	6.7	11.2	4.9
Summer—Throughfall						
Maximum (at 3 km)	10.7 (2.9)	4.8 (.4)	15.5 (3.2)	14.3 (.44)	1710	1999 (225)
At 20 km	1.0 (±.44)	.87 (±.44)	1.9 (±.75)	7.4 (±1.6)	626	626 (±142)
Background (113–129 km)	.60 (.13)	.14 (.01)	.74 (.09)	1.7 (.21)	176	160 (17)
Percent decrease at 20 km	91	82	88	48	63	69
Ratio 20 km:Background	1.7	6.3	2.6	4.3	3.6	3.9
Ratio 3 km:Background	17.8	34.8	20.9	8.3	9.7	12.5
Winter—Throughfall						
Maximum (at 3 km)	3.4 (1.3)	1.7 (.72)	5.1 (2.0)	8.8 (3.6)	1400	909 (362)
At 20 km	.38 (±.22)	.67 (±.24)	1.1 (±.44)	4.2 (±1.3)	344	344 (±112)
Background (113–129 km)	.20 (.03)	.13 (.02)	.33 (.05)	.75 (.22)	60	71 (17)
Percent decrease at 20 km	89	61	79	52	75	62
Ratio 20 km:Background	1.9	5.2	3.3	5.5	5.8	4.9
Ratio 3 km:Background	16.5	13.2	15.2	11.6	23.5	12.8
Annual—Throughfall						
Maximum (at 3 km)	14.7 (4.0)	6.7 (.8)	21.5 (4.7)	23.7 (4.5)	3111	3010 (574)
At 20 km	1.3 (±.55)	1.3 (±.52)	2.6 (±.93)	10.5 (±2.2)	874	874 (±189)
Background (113–129 km)	.81 (.12)	.27 (.03)	1.1 (.13)	2.5 (.37)	235	231 (30)
Percent decrease at 20 km	91	80	88	56	72	71
Ratio 20 km:Background	1.6	5.0	2.4	4.3	3.7	3.8
Ratio 3 km:Background	18.2	25.1	19.9	9.6	13.2	13.0

[a] Units for NH_4–N and NO_3–N are kg N ha^{-1}; SO_4–S as kg S ha^{-1}; Deposition levels at 20 km distance from the industrial center are predicted from the curve fitting equations (Fig. 3). Maximal deposition levels are from the Lysimeter site. Deposition data for the most remote sites are the average of sites JP201 (129 km; data for 2 years) and site JP213 (113 km; data for 4 years). Base cation data for the distant site are only from site JP213 and for one year. Percent decrease at 20 km is based on empirical deposition data at 3 km (Lysimeter site) in relation to predicted deposition at 20 km from the industrial center. The ratio for 20 km:Background is based on the predicted deposition at 20 km and empirical data at 113–129 km from the industrial center. The ratio for 3 km:Background is based on empirical deposition data at 3 km (Lysimtere site) and empirical data at 113–129 km from the industrial center.

[b] Base cation data are the sum of Ca^{2+} Mg^{2+} and Na^{+} expressed as eq ha^{-1}. Predicted base cation deposition at 20 km is based on the DIN + S regression equation. Standard errors could not be estimated for base cation deposition data because there was a single value for the Lysimeter site (3 km) and for the background site (113 km, JP213). The 95% confidence interval is the same as for DIN + S (see text for details).

75% in bulk and throughfall deposition at a distance of 44 and 9 km respectively, compared to distances of 94 and 15 km for NO_3–N (Fig. 3). The decline in SO_4–S and base cation deposition with distance was also greater for throughfall than for bulk deposition, but to a lesser degree than for NH_4–N and NO_3–N (Table 2; Fig. 3). Deposition of SO_4–S in bulk deposition and throughfall declined by 75% at 57 and 53 km, respectively compared to 61 and 25 km in the case of base cations (Fig. 3). The lowest deposition values in the AOSR (considered near background) were determined by averaging four years of data at site JP213 located 113 km from the industrial center and two years of data from JP201 located at a distance of 129 km (Fig. 1; Table 2). Annual average deposition of DIN and SO_4–S in throughfall at these remote sites was 1.1 and 2.5 kg ha^{-1} compared to 1.2 and 1.0 kg ha^{-1} in bulk deposition (Table 2).

The sum of measured base cation (Na, Mg and Ca) inputs in bulk deposition and throughfall were generally similar to or greater than inputs of acidic deposition in the form of DIN + S (Fig. 3). Potassium deposition was not measured because the IER columns were extracted with 1*N* KI which would have overwhelmed K from atmospheric deposition. In bulk deposition, Ca was by far the most prevalent cation (57–80% of the total), followed by Mg (14–34%), and lastly Na (4–20%). In throughfall analogous percentages were: 55–70% for Ca; 23–39% for Mg and 6–15% for Na.

Bulk deposition of NH_4–N and NO_3–N were generally higher in summer when precipitation is also greatest (Figs. 2 and 4a). In throughfall, NH_4–N deposition also tended to be higher in summer, while throughfall NO_3–N deposition was higher in summer at the highly-polluted AMS-5 and Lysimeter sites, but not at other sites.

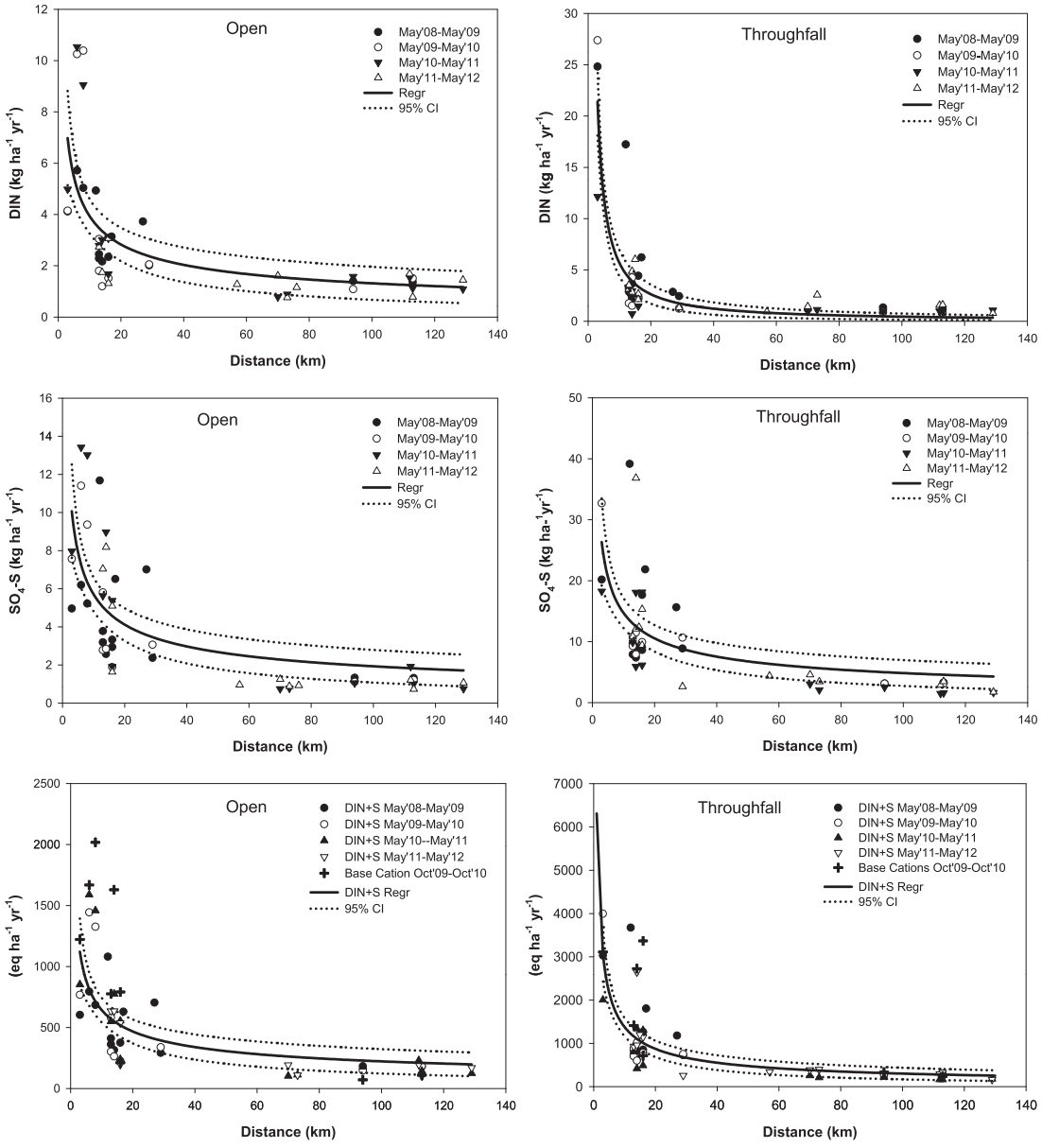

Fig. 3. Deposition (kg ha^{-1} yr^{-1}) of dissolved inorganic N (DIN; sum of NO_3–N + NH_4–N) and SO_4–S in forest clearings and in throughfall versus distance from the industrial center of the Athabasca Oil Sands Region. Also shown are four years of DIN + SO_4–S deposition (eq ha^{-1} yr^{-1}) in forest clearings and in throughfall versus distance. On these latter two graphs, data points (as + symbols) are shown (but not a separate regression line) for one year of base cation deposition (Na + Mg + Ca). The regression line for DIN + SO_4–S deposition was also used to predict base cation deposition with distance (see text for details).

Throughfall SO_4–S deposition was variable between summer and winter with no clear pattern (Fig. 4b).

3.2. Comparison of reduced and oxidized N forms

With a few exceptions ammonium to nitrate ratios (NH_4–N:NO_3–N) in bulk deposition and in throughfall were >1 in the summer. Ratios ranged from .3 to 7.6, indicating that deposition of NH_4–N is nearly always greater than deposition of NO_3–N in summer. In winter, NH_4–N:NO_3–N ratios in bulk deposition were generally several-fold lower than in summer. A similar pattern was observed in throughfall, although in several instances winter throughfall ratios ranged from 3 to 5. The average NH_4–N:NO_3–N ratios for annual bulk deposition and throughfall, considering all years and sampling locations were 1.8 and 2.0, respectively, indicating that over the monitoring network deposition of NH_4–N was approximately double that of NO_3–N (Fig. 4). The highest NH_4–N:NO_3–N ratios in bulk deposition during summer were found at the Peat Pond and W1 sites located six and eight km from the industrial center; winter ratios at these sites were also among the highest. However ratios in bulk deposition in winter only occasionally exceeded 2.0.

3.3. Relationship between gaseous pollutants and atmospheric deposition of N and S

In summer atmospheric concentrations of gaseous pollutants declined in this order: NH_3 > SO_2 > NO_2 > HNO_3. In winter concentrations declined in this order: NO_2 > SO_2 > NH_3 > HNO_3. Concentrations of the first three pollutants listed occurred within the same relative ranges, but concentrations of HNO_3 were generally close to an order of magnitude lower than the other three gaseous

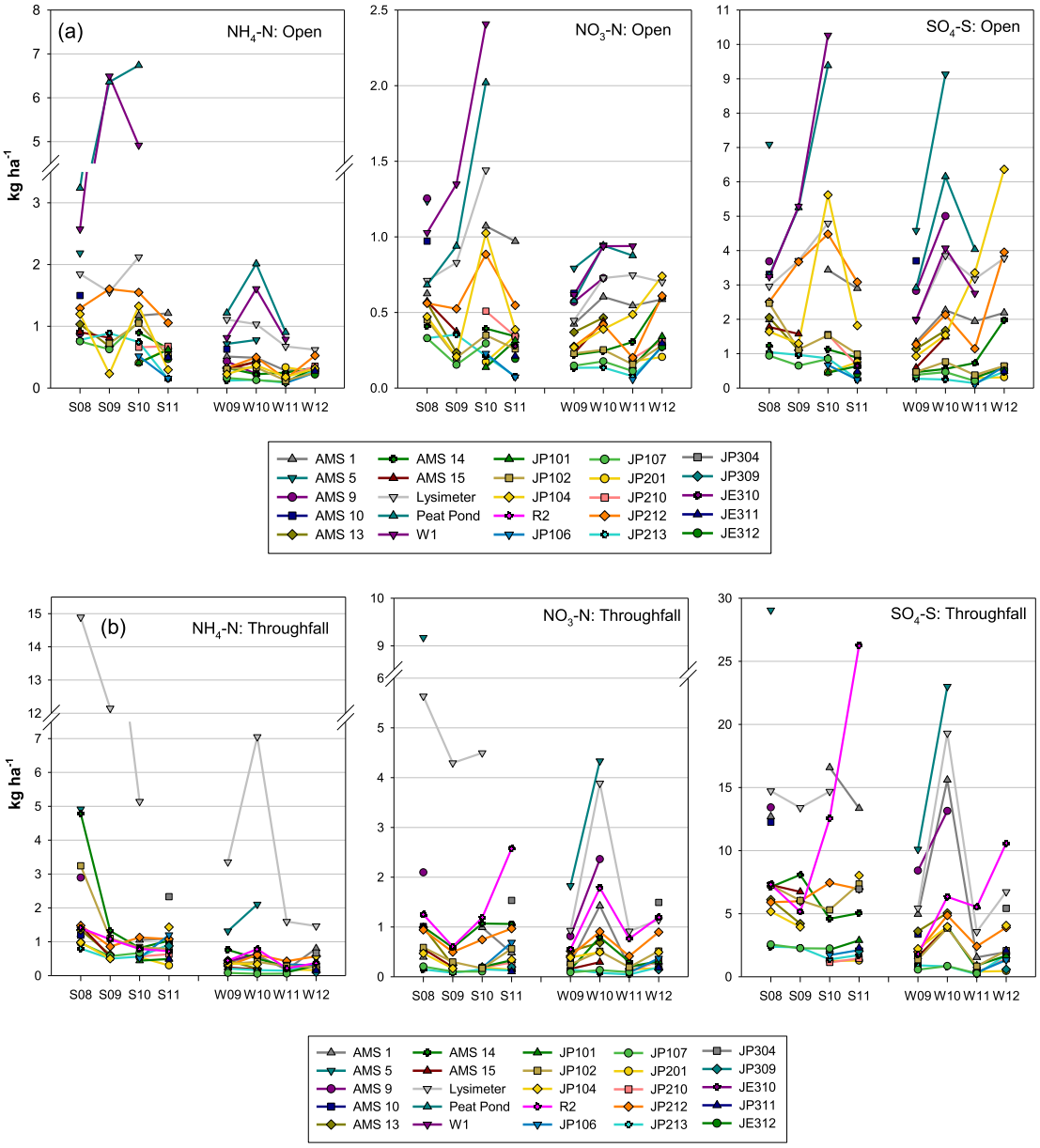

Fig. 4. Temporal patterns of summer and winter deposition of NH_4–N, NO_3–N and SO_4–S in (a) forest clearings (open) and (b) throughfall under jack pine in the Athabasca Oil Sands Region.

pollutants (Fig. 5). Correlations between atmospheric concentrations of NO_2 and deposition fluxes of NO_3–N measured with the IER samplers were stronger and more consistent in winter compared to summer and stronger in collectors in forest clearings (bulk deposition) compared to throughfall collected under tree canopies (data not shown). Deposition of NO_3–N in bulk deposition ($R^2 = .39$, $p < .001$) and throughfall ($R^2 = .23$, $p = .005$) were correlated with NO_2 concentrations during the winter, the period when average NO_2 concentrations were 2–3 times greater than in summer. Including HNO_3 in the regressions did not improve the relationship, suggesting that HNO_3 was not a major driver of NO_3 deposition, presumably because of the relatively low concentrations of HNO_3 in the AOSR. In summer, throughfall and bulk deposition of NH_4–N were correlated ($p > .001$) with NH_3 concentrations, largely because of industrial site values that dominated the linear regression relationship at high deposition and concentration values at the high end of the *y*- and *x*-axis ranges (data not shown). In winter relationships were weak (R^2 values of .08–.12, $p = .01$–.06).

The relationship between deposition of DIN (NO_3–N + NH_4–N) and atmospheric concentrations of the sum of NO_2, HNO_3 and NH_3 (expressed as N) in summer was insignificant in open areas ($R^2 = .05$; $p > .1$; Fig. 6a) and weakly significantly in throughfall ($R^2 = .17$; $p = .03$; Fig. 6b). In winter relationships were stronger ($R^2 = .59$, $p < .001$ in open and $R^2 = .25$, $p = .003$ in throughfall; Fig. 6). Bulk deposition of SO_4–S was more strongly correlated with atmospheric SO_2 concentrations in summer ($R^2 = .37$, $p < .001$) than winter ($R^2 = .15$, $p = .03$). In throughfall deposition of SO_4–S was weakly correlated with SO_2 concentrations in winter and summer ($R^2 = .15$–.18, $p = .02$–.03; Fig. 6).

3.4. Effects of forest fires on pollutant deposition and concentrations

In early summer of 2011 extensive forest fires occurred in the region with 806,055 ha burned compared to the 10-yr average of 195,726 ha burned (Government of Alberta, Environment and

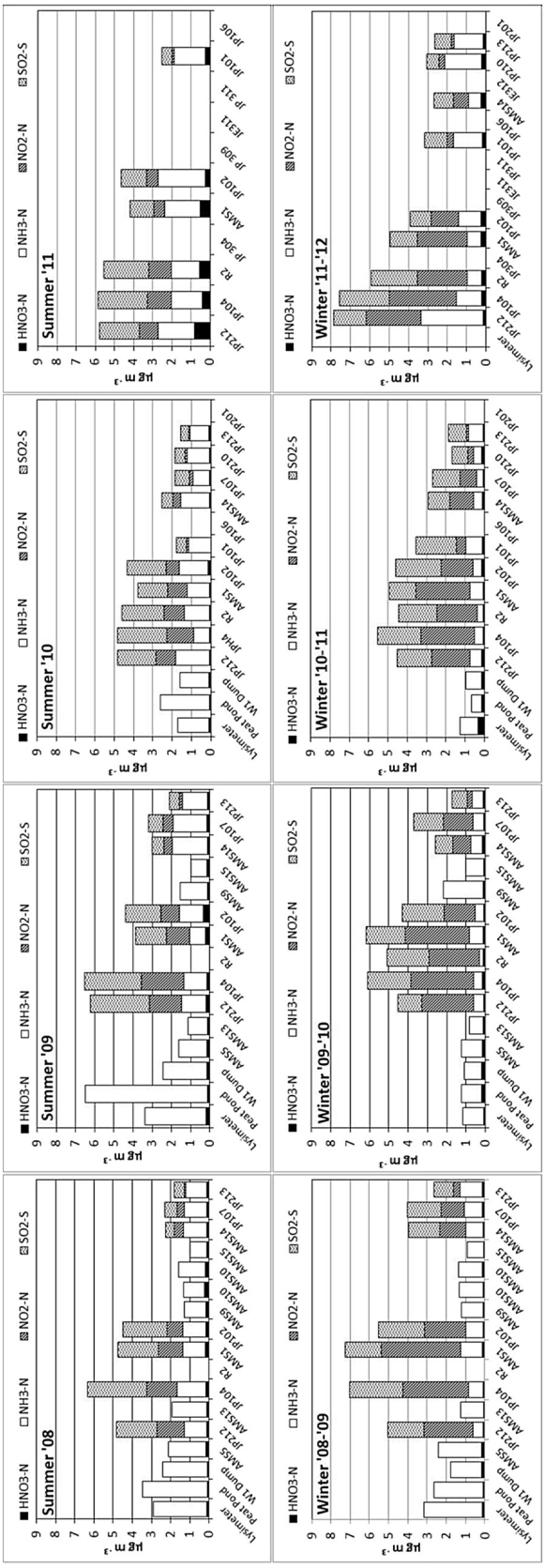

Fig. 5. Seasonally-averaged atmospheric concentrations of HNO_3, NH_3, NO_2 and SO_2 (μg N or S m^{-3}) for the same monitoring sites where atmospheric deposition was measured with ion exchange resin throughfall samplers. Data for gaseous pollutant concentrations are from passive samplers. Note that for some sites NO_2 and SO_2 were not measured. See text for passive sampling methods used.

Sustainable Resource Development http://srd.alberta.ca/Default.aspx; http://esrd.alberta.ca/wildfire/wildfire-status/historical-wildfire-information/10-year-statistical-summary.aspx). A massive fire complex north of Fort McKay and Fort McMurray, encompassing 700,000 ha, burned from mid-May and into June 2011 (Fig. 1). In January to March 2012 two wood burning events were carried out; one to the west of the AMS15 site and one to the east of AMS1 (Fig. 1). Evidence of fire effects on throughfall chemistry were observed most clearly at the R2 site, with less dramatic deposition increases at nearby sites, including JP104, JP102, JP304 and JP212. At R2 throughfall SO_4–S deposition in summer 2011 increased by 215% compared to the 2008–2010 summer average, and increased by 76% at JP104, 19% at JP102, and 8% at JP212. However, during summer 2011 bulk deposition of SO_4–S in forest clearings declined at JP104 and most nearby sites compared to the previous summer (Fig. 4a). In contrast, bulk deposition of SO_4–S at JP104 and JP212 in winter 2012 was 228 and 161% higher than the average of the previous three winters. A similar trend was observed for JP101, AMS14 and JP106 where bulk deposition of SO_4–S was 106, 240 and 500% greater in winter 2012 compared to previous winters (Fig. 4a). Deposition of SO_4–S in throughfall in winter 2012 was double that of winter 2009 and 2011 but similar to deposition in winter 2010; thus it isn't clear to what degree fire emissions affected throughfall SO_4–S deposition in winter 2012.

Throughfall NO_3–N deposition at R2 in summer 2011 increased by 154% compared to the previous three summers (Fig. 4b). Throughfall deposition of NO_3–N appear to also be elevated at nearby JP304 in summer 2011 and in winter 2012 compared to nearby sites, although only one summer and winter of data are available for this site. Bulk deposition of NO_3–N also appear higher than normal in winter 2012 at JP104, JP212, AMS14, JP213, JP101 and JP106 (only two data points for the last two sites, however), suggesting a possible influence of the wood burning fires that occurred in January to March 2012 (Fig. 4a).

Throughfall deposition of NH_4–N in summer 2011 was somewhat higher than expected (based on previous years and site location) at JP104, JP304 and possibly JP106. In winter 2012 throughfall deposition of NH_4–N at AMS1 was 34–370% higher than in previous winters (Fig. 4b). Deposition of NH_4–N in forest clearings was not affected by fire emissions in summer 2011 and in winter 2012 our data are insufficient to detect a clear increase compared to previous years. Detectable increases in N or S deposition following the widespread fires in summer 2011 as mentioned above, were nearly always restricted to monitoring sites clustered near the AMS1, R2, JP212 and JP304 sites (Figs. 1 and 4). One exception is site JP106, which is located within the perimeter of the wildfire.

Atmospheric concentrations of HNO_3 in summer 2011 were on average three-fold higher than in summers from 2005 to 2010 and HNO_3 concentrations in winter 2012 were double those of the previous six winters (Including unpublished data from larger network; data not shown). Concentrations of NH_3 also increased by 50% in summer 2011 compared to the previous six summers, and increased 25% in winter 2012 compared to previous winters. Concentrations of NO_2 and SO_2 did not increase in summer 2011 nor in the following winter.

4. Discussion

4.1. Spatial and seasonal patterns of deposition for N, S and base cations

Reports of a number of pollutants and receptors indicate a common spatial pattern in the AOSR of rapidly decreasing pollution deposition or accumulation with distance from the primary source

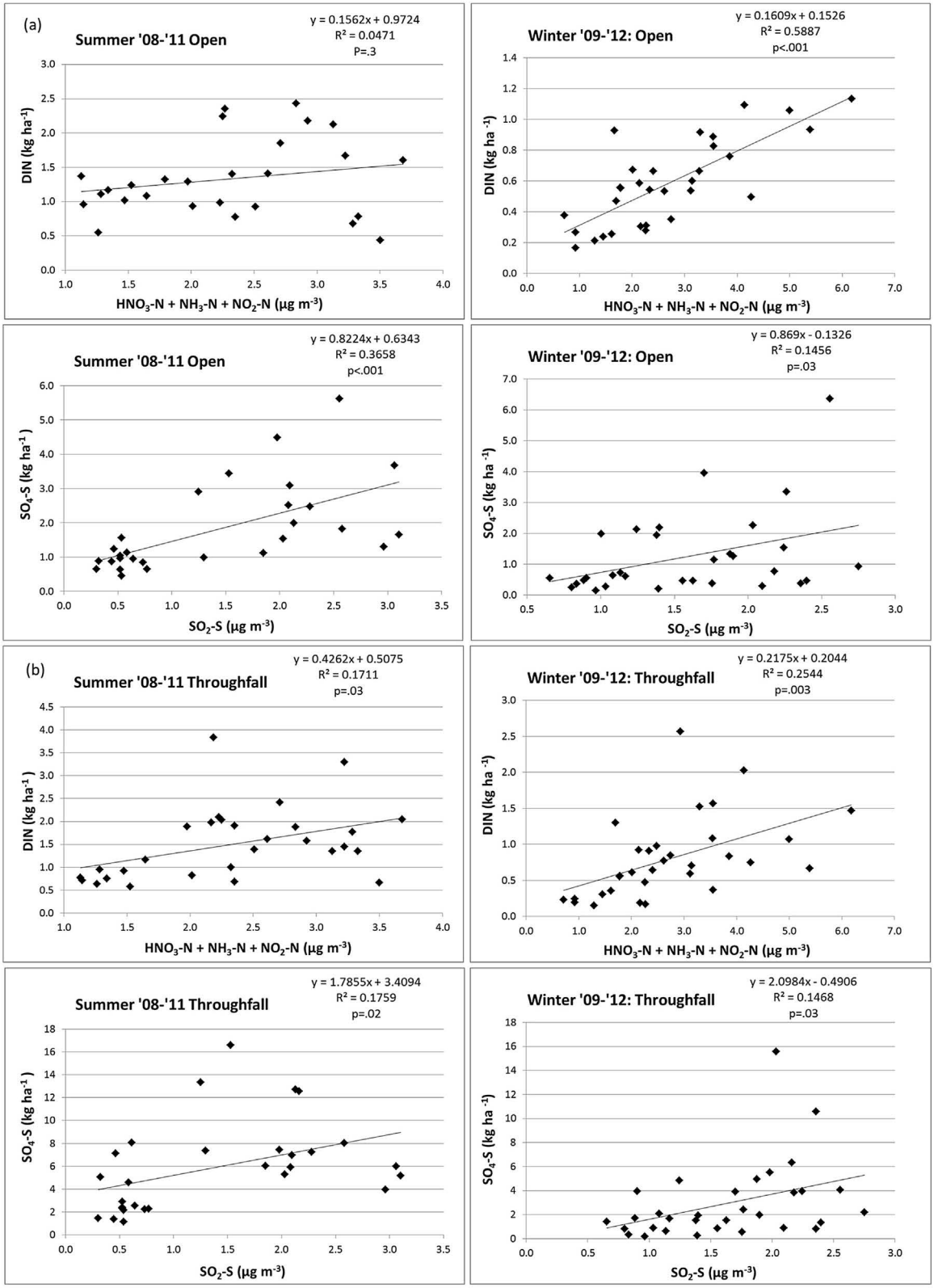

Fig. 6. Linear correlation between the sum of the average atmospheric concentrations of HNO_3—N, NH_3—N and NO_2—N from passive samplers versus bulk deposition (open sites) of DIN (NO_3—N + NH_4—N); also shown are average concentrations of SO_2 versus deposition of SO_4—S in open areas (a). Analogous correlations for throughfall under jack pine canopies are shown in b. Data are shown for the summer and winter seasons. Data were combined from the four years of the study (May 2008 to May 2012).

area. For example, concentrations of aluminum, vanadium, lead and total polycyclic aromatic hydrocarbons (PAHs) in the lichen *Hypogymnia physodes* collected from trees in the AOSR show the same pattern of steeply declining values within 25 km of the industrial zone (Graney et al., 2012; Studabaker et al., 2012), highly similar to the spatial pattern reported herein for throughfall deposition of NH_4–N, NO_3–N and base cations. Simulated deposition of oxidized N pollutants and of S pollutants from the CALPUFF model, and concentrations of N and S in two epiphytic lichen species (*H. physodes* and *Evernia mesomorpha*) also followed this same spatial pattern with distance from the industrial center (Davies, 2012). Similarly, ratios of $^{207}Pb/^{206}Pb$ increased exponentially with distance from the industrial center (Graney et al., 2012).

In source apportionment studies in the AOSR the most important source categories influencing the chemistry of epiphytic lichens were oil sand and processed material, tailing sand fugitive dust, combustion processes, limestone and haul road fugitive dust, and a general urban source. Receptor modeling with epiphytic lichens indicated that the contribution of each of these sources decreased exponentially with distance from the industrial center, with a major dropoff within 20 km of the source area (Landis et al., 2012). Considering that dust is the likely source of the base cations measured in deposition with the IER samplers, the results of Landis et al. (2012) are in strong agreement with the IER deposition data (Fig. 3). Likewise, emissions from the processing of oil sand materials, the presumed major source of N and S emissions, in the area encompassing the primary industrial center are in agreement with the spatial pattern for deposition of N and S reported in this study (Fig. 3).

CALPUFF modeled deposition of oxidized N in the AOSR is in general agreement with throughfall deposition of NO_3–N. The model simulated dry and wet deposition to the forest canopy and thus can be compared to throughfall data. Throughfall and simulated deposition both show maximum NO_3–N deposition of ca. 10 kg $ha^{-1}yr^{-1}$ near the industrial center. In the more remote sites (e.g., >30 km from the industrial center) throughfall deposition of NO_3–N was typically .5 kg ha^{-1} yr^{-1}, although values were occasionally closer to 1 kg ha^{-1} yr^{-1}. By comparison CALPUFF predicted that NO_3–N deposition was approximately 1.5 kg ha^{-1} yr^{-1} even at a distance of 145 km from the center.

One cause of the lower throughfall NO_3–N deposition compared to the CALPUFF predictions may be due to canopy uptake of NO_3 from wet deposition, which results in greater than expected underestimates of NO_3–N deposition (Fenn et al., 2013). Many studies have reported preferential canopy uptake of NO_3 from wet deposition compared to NH_4–N uptake (Freedman and Prager, 1986; Johnson and Lindberg, 1992; Lovett and Lindberg, 1993). This phenomenon is widespread in the Pacific Northwest region of North America (Edmonds et al., 1995; Fenn et al., 2013; Klopatek et al., 2006) and is characterized by greater wet or bulk deposition of NO_3–N in forest clearings than in throughfall under the forest canopy in sites with low to moderate air pollution exposure. Preferential canopy consumption of NO_3 has been reported in remote jack pine stands in the AOSR (Fenn et al., 2013).

Simulated background NO_3–N deposition in the AOSR ranged from 1.0 to 1.8 kg ha^{-1} yr^{-1} (Davies, 2012). Highest simulated background deposition of NO_3–N and of SO_4–S was in the southwestern end of the region, which is closer to the distant urban emissions sources to the south. Simulations of deposition of reduced forms of N (NH_x), either as background or as influenced by emissions sources in the AOSR were not performed (Davies, 2012). By comparison, the estimated background NO_3–N deposition based on throughfall measured at sites located 113–129 km from the center, and accounting for canopy consumption of wet-deposited NO_3–N (Fenn et al., 2013), was .9 kg ha^{-1} yr^{-1}. Combining the background throughfall deposition of NH_4–N (.8 kg ha^{-1} yr^{-1}) we calculate a N deposition background of 1.7 kg ha^{-1} yr^{-1}. Background bulk deposition (composed mainly of wet deposition) of N in forest clearings was 1.2 kg ha^{-1} yr^{-1} (Table 2).

CALPUFF modeled SO_4–S deposition values were much lower than throughfall SO_4–S deposition. Peak values in the industrial zone were 33–39 kg S ha^{-1} yr^{-1} as throughfall compared to 9–13 in the Calpuff model output (Davies, 2012) – approximately a three-fold difference. At more remote sites (57–129 km distant) throughfall SO_4–S deposition ranged from 1.5 to 4.6 kg ha^{-1} yr^{-1}) except for the AMS 14 site (74 km) where values ranged from 5 to 12 kg ha^{-1} yr^{-1}, due to additional local S emissions. By comparison, over the same distance from the industrial center, simulated S deposition ranged from 2.0 to 2.9 kg ha^{-1} yr^{-1} (Davies, 2012). The apparent model underestimates of S deposition may be at least partially explained by model-predicted underestimates for the top 25 1-h average SO_2 concentrations in the study region (Davies, 2012), and likely underestimates of particulate SO_4–S deposition.

Simulated background SO_4–S deposition ranged from 1.4 to 2.1 kg ha^{-1} yr^{-1} compared to estimated background deposition of 1.0 and 2.5 kg S ha^{-1} yr^{-1} in bulk deposition and throughfall (Table 2). Thus, in contrast to NO_3–N, simulated background S deposition was lower than but similar to the throughfall estimated background. This is likely due in large part to the fact that a large proportion of atmospheric SO_4–S is transported much further from the source area compared to DIN as shown herein.

Enrichment of N, S and base cations in bulk deposition and throughfall were all similar (2–5 fold) at 20 km distance from the industrial center. Likewise, enrichment of N and S in bulk deposition were similar at 3 km (4–7 fold), except for base cations which were enriched 11-fold at 3 km (Table 2). However in throughfall at 3 km distance, deposition of NH_4–N, NO_3–N and DIN was 18–25 times greater than background, while SO_4–S and base cations were 10 and 13 times over background. These comparisons suggest that in stands adjacent to the industrial source area, dry deposition of N to the forest canopy occurs at high rates resulting in elevated N deposition. However, at a distance of 20 km from the industrial core N deposition in throughfall and in open areas has already decreased greatly, resulting in similar enrichment factors for all the ions measured in this study (Table 2).

Deposition in throughfall of NO_3–N and NH_4–N were reduced by 80 and 91% at 20 km from the industrial center demonstrating the rapid dropoff with distance from the source area. In contrast throughfall deposition of base cations and SO_4–S only decreased by 72 and 56% at 20 km and by 75% at 25 and 53 km, illustrating the larger footprint of SO_4–S, and to a lesser degree, of base cation deposition in the AOSR. However, the percent decrease in bulk deposition of base cations at 20 km from the industrial center (62%; Table 2) is greater than for the other ions measured, suggesting that fallout of cations from fugitive dust in forest clearings is more rapid than that of N and S pollutants. The greater spatial extent of S deposition is likely due to long distance transport of aerosols composed of SO_4 and base cations, or formation of such aerosols during atmospheric transport. It may also be due to the lower deposition velocity of SO_2 and SO_4^{2-} (typical values of .5–.7 cm s^{-1}) compared to NH_3 and HNO_3 (typical values of 1.5–3.5 cm s^{-1}). However, the deposition velocity of NO_2 (typically ca. .3 cm s^{-1}) is also relatively low (Brook et al., 1999; Flechard et al., 2011; Horváth, 2003; Pratt et al., 1996; Puxbaum and Gregori, 1998; Voldner et al., 1986; Zhang et al., 2009). Throughfall deposition of NH_4–N was generally higher in summer when atmospheric NH_3 concentrations were also higher. However, much of the throughfall NH_4–N deposition may be due to deposition of particulate NH_4, such as ammonium sulfate.

4.2. Comparison of reduced and oxidized N forms

Historical emphasis on N monitoring, modeling and effects in the AOSR has focused almost exclusively on oxidized forms of N. This is evidenced by N and S deposition modeling work that includes only NO_x and SO_x (Davies, 2012). However, our deposition data clearly show that atmospheric inputs of N in reduced forms are greater than oxidized forms. Atmospheric concentrations of gaseous NO_y and NH_3 in the AOSR are both elevated; however, much of the reduced N input in the region is likely in particulate form as evidenced by stack emissions (Wang et al., 2012; Watson et al., 2011) and the steeply declining patterns of deposition with distance from the source zone.

Although deposition of NH_4–N is on average double that of NO_3–N deposition in the AOSR, emissions inventories of the National Pollutant Release Inventory (NPRI, 2010, 2011) report that NH_3 emissions from stationary sources were only 3% as large as NO_2 emissions in 2010 and 2011. Furthermore, the NPRI inventory does not include NO_x emissions from mobile sources, which in 2008 made up 40% of the anthropogenic NO_x emissions in the AOSR (Davies, 2012). The discrepancy between the reported dominance of NO_x emissions and deposition data showing that NH_4–N deposition is double that of NO_3–N deposition is apparently due to unreported elevated emissions of particulate NH_4 and likely also because of underestimates in reported NH_3 emissions. Emissions of particulate matter mass is reported in the emissions inventory (NPRI, 2010, 2011), but chemical characterization of particulate matter emissions is not.

Short-term analyses of the chemical composition of the emissions from three stacks in two facilities that are among the largest stationary sources in the AOSR illustrate the importance of particulate NH_4 and SO_4 emissions in the region (Wang et al., 2012). On a molar basis, the NH_4 to SO_4 ratio in $PM_{2.5}$ was approximately 2 in stacks A and B, indicative of fully neutralized $(NH_4)_2SO_4$ (Wang et al., 2012). In summer 2008 NH_3 emissions were elevated (86 kg h^{-1}) in Stack B at Facility A that is equipped with a SO_2 scrubber (a diluted slurry of $(NH_4)_2SO_4$ containing an excess of NH_3 to produce $(NH_4)_2SO_4$ fertilizer) as part of a flue gas desulfurization system. In Stack B, emissions of NH_3 (86 kg/h) and NO_x (132 kg/h) were of the same order of magnitude (Wang et al., 2012); although in this and other comparisons of reduced and oxidized N compounds, comparisons are more appropriately made on a molar or N-content basis.

Although routine analyses of particulate N and S emissions are not available, chemical analysis of the stack emissions indicate that the amounts and N forms emitted from the stacks vary widely depending on feedstocks, petrochemicals and processes. For example, from short-term summer and winter samplings of stack emissions, 5 and 44% of the N emitted was in reduced form from Stacks A and B respectively (Watson et al., 2011). The major particle component was ammonium sulfate in Stacks A and B, and sulfuric acid for Stack C (Wang et al., 2012). In summer and winter emissions of S and oxidized N were dominated by gaseous emissions. Emissions of reduced N in summer were mainly in gaseous form, but in winter particulate NH_4 emissions were much greater (Watson et al., 2011). The tailings ponds near AMS2 are known to be a point source of NH_3 emissions (NPRI, 2011) and we have confirmed this with passive sampler data showing long-term average NH_3 concentrations at AMS2 that are approximately three times higher than typical values for the AOSR (Andrzej Bytnerowicz, unpublished data).

In summary, publicly available N emissions data for the AOSR are inadequate to address quantitatively what sources and processes are responsible for the observed atmospheric deposition in throughfall and bulk deposition. However, it is clear that emissions and atmospheric deposition of reduced forms of N (NH_3 and NH_4^+) are much greater than previous understanding and available emissions inventories indicate.

4.3. Potential ecological effects of air pollution in the AOSR

The mean of the 25-top 1-h SO_2 concentrations during each year at three air monitoring stations within 12 km of the main industrial area from 2004 to 2007 ranged from 226 to 400 μg m^{-3} (Davies, 2012). These peak SO_2 values are within the range at which sensitive lichen species can be affected by short term SO_2 exposures (ca. 200–400 μg m^{-3}; Nash and Gries, 2002; Sanz et al., 1992). In a previous study, net CO_2 assimilation rate was significantly reduced in *E. mesomorpha*, a common epiphytic lichen species in the AOSR, by exposure to 223 μg SO_2 m^{-3} for periods as short as one hour (Huebert et al., 1985). *E. mesomorpha* is among the lichen species that are most responsive to SO_2 exposure (Fields, 1988). In contrast, annual average SO_2 concentrations in the AOSR (1–8 μg m^{-3}; Davies, 2012), are generally below the levels at which effects on lichens or lichen communities have been commonly reported (20–130 μg m^{-3}; Häffner et al., 2001; Huebert et al., 1985; LeBlanc and Rao, 1975; McCune, 1988).

Concentrations of N in foliage of *P. banksiana* and in the lichen species *E. mesomorpha* and *H. physodes* were positively correlated with atmospheric concentrations of NO_2 (Laxton et al., 2010), indicating that N deposition in the AOSR enriches the N status of vegetation and lichens (Davies, 2012) in the more polluted portions of the AOSR. Likewise, a 2004 survey of the TEEM plots revealed that S concentrations in foliage of *P. banksiana* (total S and inorganic S) and of the forest floor, and both N and S levels in lichen tissue, increased with increasing atmospheric deposition (Jones and Associates Ltd., 2007). Further work is needed to evaluate possible biological responses to this N and S enrichment and its spatial extent.

Although soils in jack pine stands are naturally acidic with low base cation saturation, the consensus of previous studies in the AOSR is that there is limited potential for acidification of soils or lakes under current conditions (Hazewinkel et al., 2008; Jung et al., 2013; Whitfield et al., 2009). A field study at four forest sites in the AOSR found that soil pH increased from 2005 to 2010. The authors proposed that likely mechanisms for the soil pH increase were decreased H^+ input as a result of decreasing S deposition and increased base cation deposition (Jung et al., 2013). The results of our study also indicate that base cation deposition closely tracks acidic deposition in the form of N and S deposition. Watmough et al. (2014) concluded that despite extremely low soil base cation weathering rates in the region, the risk of soil acidification is mitigated to a large extent by high base cation deposition.

4.4. Relationship between gaseous pollutants and atmospheric deposition of N and S

The strongest relationships between deposition inputs and atmospheric concentrations of NO_2, SO_2, and the sum of gaseous N pollutants (NO_2, NH_3 and HNO_3) were found in open sites. Canopy interactions, including canopy uptake of N and S pollutants and the accumulation in the canopy of N and S compounds including particulate pollutants (Hertel et al., 2012; Lovett and Lindberg, 1993), likely confounded relationships between levels of gaseous pollutants and throughfall fluxes. In the case of NH_3 concentrations in relation to NH_4–N deposition during summer, these were correlated in throughfall and open areas, but the regressions were strongly influenced by high levels of atmospheric NH_3 and NH_4–N deposition during summer periods at the industrial sites. In contrast, the relationship between NO_2 and NO_3–N deposition in

open areas and the sum of nitrogenous gases and DIN deposition in open areas were strongest in winter, when NO_2 concentrations were 2–3 times higher than in summer. Correlations between bulk deposition of SO_4–S and SO_2 concentrations were greater in summer than winter, although the mechanism behind this isn't known. We speculate that it could be related to greater deposition of $(NH_4)_2SO_4$ in summer when NH_4–N deposition is greatest.

It seems clear that gaseous N and S compounds are important drivers of atmospheric deposition in the AOSR. However in summary, the sometimes weak correlations between gaseous pollutants and deposition may be due to the following: (1) A significant portion of the dry deposition is a result of particulate deposition, including pollutants that are directly emitted from industrial stacks as particulates (e.g., as ammonium sulfate; Wang et al., 2012; Watson et al., 2011); (2) Canopy interactions with dry and wet deposited pollutants confound these relationships, and (3) Gaseous deposition isn't efficiently deposited to open site collectors. Which form of deposition (i.e., gaseous or particulate) is predominant at any given time or location may differ based on varying emissions mixtures of gaseous and particulate forms and meteorological conditions. Further work is needed to draw definite conclusions regarding the primary drivers of N and S deposition in the AOSR, including a better understanding of how the compounds involved in deposition may differ spatially and temporally within the region.

4.5. Effects of forest fires on pollutant deposition and concentrations

In summer 2011 fire emissions were primarily from a large wildfire located ca. 100 km north of Ft. McMurray that began in mid-May and burned for several weeks. In winter 2012 fire emissions were from two planned wood burnings that occurred between January and March, one just west of AMS15 and one to the east of AMS1 (Fig. 1). Regarding evidence of fire emissions in throughfall, spikes in SO_4–S deposition were prominent at the cluster of sites near R2, followed by much lower increases in deposition of NO_3–N and NH_4–N. This study was not designed to study fire effects on deposition inputs. A more dense network of deposition samplers with shorter sampling intervals would likely have improved the detection of fire effects on deposition. Furthermore, increased N and S deposition from fire emissions may be obscured in the more polluted sites because of the already high deposition fluxes at such sites. Nonetheless, we found a hotspot of deposition effects in throughfall from the fire in a cluster of sites including the R2, JP212, JP104, and JP304 sites. Winds in summer from the fire region to the north were sufficient to account for smoke transport to the cluster of sites surrounding R2, and satellite photos illustrated that smoke emissions spread widely over the sampling network in the AOSR.

Secondary sulfate is the most abundant inorganic ion found in smoke plumes from biomass burning and is a key tracer species of fire emissions (Garcia-Hurtado et al., 2014; Reid et al., 2005). Ammonium and nitrate particles are also produced in aged smoke plumes but in lesser amounts, as reported in this study. Much of the particle formation containing these three ions is from primary gas emissions from fire of SO_2, NO_x and NH_3 (Reid et al., 2005). We presume that the major fire inputs to the bulk deposition samplers in the AOSR was in the form of secondary aerosols from the smoke plumes and that the strong SO_4–S signal in bulk deposition in winter 2012 and in summer 2011 throughfall is a result of S emissions from burned biomass. The forest fire functioned as a release agent of the S and N that accumulated in these fuels. Hecobian et al. (2011) reported that NO_3, NH_4 and SO_4 aerosols in smoke emissions are higher when influenced by urban emissions (see also Hegg et al., 1987). Presumably, emissions from industrial activities in the AOSR would also result in increased levels of N and S aerosols in smoke emissions, especially from burned areas within 20–30 km of the industrial center, or possibly further in the case of SO_4.

Data from passive samplers indicate that concentrations of NH_3 and HNO_3 at sites near R2 in summer 2011 when extensive forest burning occurred were 12–48% and 2–8 times higher respectively than in previous summers. The increased HNO_3 concentrations measured with passive samplers during the fires in the AOSR in 2011 are likely from nitrous acid (HNO_2) emitted from the fires. Nitrous acid has been shown to occur at elevated levels during fire events in the Sierra Nevada of California, USA (Bytnerowicz et al., 2002).

It seems counterintuitive that throughout the monitoring network, bulk deposition of NO_3–N, NH_4–N and SO_4–S in summer 2011 did not increase in response to fire as throughfall deposition did at the R2 and surrounding sites. In the case of NO_3–N and NH_4–N deposition this may have partially been because of the importance of increased concentrations of gaseous pollutants from summertime high-temperature fire emissions that are not collected by the open funnel collectors. However, postfire throughfall SO_4–S deposition increased much more than NO_3–N or NH_4–N, and yet SO_2 concentrations decreased at nearly all sites during summer 2011, suggesting throughfall SO_4 deposition was mainly from canopy accumulation of particulates from fire emissions as the literature attests (Garcia-Hurtado et al., 2014; Reid et al., 2005). Thus, we speculate that the lack of increased N or S deposition in bulk collectors in summer 2011 was because of the relatively dry climate and dry summer in 2011 (Fig. 2) resulting in inefficient washout of pollutants to funnel collectors in open sites, and possibly because much of the wildfire smoke plume was at higher elevation than the open funnel collectors located at ground level. On the other hand, aerosols and gases in the wildfire smoke plume were likely both intercepted by the forest canopy, thus affecting summer throughfall deposition fluxes (Fig. 4b).

In contrast to the summer 2011 results, bulk deposition of NO_3–N, NH_4–N and SO_4–S all increased in winter 2012 at the R2 cluster of sites in addition to several more distant sites. We hypothesize that this is a result of fallout of smoke aerosols from lower elevational plumes to the bulk collectors from the smaller, less intense, and slower-burning controlled “wood-burning” fires during winter.

The postfire increase in throughfall NO_3–N deposition in summer 2011 at R2 was presumably partially driven by the 9-fold increase in HNO_3/HNO_2 at R2. However, NO_3 in particulate matter could have also contributed to throughfall NO_3–N deposition. Concentrations of NO_2 decreased at all the sites in summer 2011 except for a modest 14% increase at R2. Bulk deposition of NO_3–N in forest clearings decreased in the same region further suggesting that particulate deposition wasn't the main driver of NO_3–N deposition in summer 2011. In winter 2012 there was no clear signal of increased throughfall NO_3–N deposition, but bulk deposition increased sharply at JP104, JP212 and several other sites. Winter time concentrations of NO_2 and HNO_3 increased by 12–30% and 44–127% at the R2 cluster of sites, which is much lower than the 9-fold increase in HNO_3/HNO_2 at R2 in summer. Thus, it seems that particulate emissions from the lower intensity wood burning were a larger driver of fire-induced increases in wintertime NO_3 deposition than were gaseous emissions.

In summer 2011 NH_4–N deposition in throughfall increased 2-fold at two of the sites adjacent to R2, while NH_3 concentrations increased 12–48%. In winter 2012, NH_3 concentrations at the R2 cluster of sites increased 2–6 fold and throughfall deposition of NH_4–N doubled at AMS1 near the wood pile burning, and increased to a lesser degree at some sites near R2. However, a longer period of monitoring and a denser network is needed to

quantify to what degree NH_4–N deposition increased due to fire. We conclude that throughfall NH_4–N deposition was enhanced postfire by increased NH_3 and particulate matter accumulation in the canopy. Bulk deposition of NH_4–N in winter 2012 may have increased slightly because of fire exposure, but our data are insufficient to detect a clear increase compared to previous years.

5. Conclusions

As noted previously for other pollutants, throughfall deposition of NO_3–N and NH_4–N decreased exponentially within a 20–25 km zone surrounding the industrial center. At a distance of 20 km from the industrial center throughfall N deposition decreased by 88%, while S and base cations decreased by 56 and 72% respectively, showing a greater footprint. Deposition of NH_4–N was on average double that of NO_3–N. Higher deposition of reduced forms of N compared to oxidized forms had not previously been well documented except for data showing elevated atmospheric concentrations of NH_3 in the AOSR (Bytnerowicz et al., 2010a,b). More studies are needed to better understand the emissions sources and chemical forms of reduced N that contribute to NH_4–N deposition in the region. Results of this study support the hypothesis that eutrophication effects to sensitive organisms may be of greater concern because acidic deposition is matched by equivalent amounts of base cation deposition (Watmough et al., 2014). However, the zone at risk of excess N effects may be limited in size as indicated by the steep decrease in N deposition with distance from the source areas. When fires occur in this boreal zone it results in increases in atmospheric concentrations of HNO_3 and NH_3 and increased deposition of SO_4–S, but much lesser increases in deposition of NO_3–N and NH_4–N. The postfire increase in SO_4–S deposition appears to be primarily from increased particulate S deposition, while increased N deposition is likely a result of increases in gaseous and particulate forms of N from fire.

Acknowledgments

This work was funded by the Wood Buffalo Environmental Association, Fort McMurray, Alberta, Canada. The authors thank Kevin Percy, Veronica Chisholm, Ted Sutton, Ken Foster, Carna MacEachern, Dorothy Brown, Natalie Bonnell, Evan Magill, Sarah Eaton, Amanda Horning, Bonnie Bartlett,Yu-Mei Hsu, Justin Straker, and Jean-Guy Zakrevsky for guidance and help with field work and logistics in carrying out this work.

References

Asman, W.A.H., Ridder, T.B., Reijnders, H.F.R., Slanina, J., 1982. Influence and prevention of bird-droppings in precipitation chemistry experiments. Water Air Soil Pollut. 17, 415–420.

Bleeker, A., Draaijers, G., van der Veen, D., Erisman, J.W., Mols, H., Fonteijn, P., Geusebroek, M., 2003. Field intercomparison of throughfall measurements performed within the framework of the Pan European intensive monitoring program of EU/ICP Forest. Environ. Pollut. 125, 123–138.

Brook, J.R., Zhang, L., Li, Y., Johnson, D., 1999. Description and evaluation of a model of deposition velocities for routine estimates of dry deposition over North America. Part II: review of past measurements and model results. Atmos. Environ. 33, 5053–5070.

Bytnerowicz, A., Tausz, M., Alonso, R., Jones, D., Johnson, R., Grulke, N., 2002. Summer-time distribution of air pollutants in Sequoia National Park, California. Environ. Pollut. 118, 187–203.

Bytnerowicz, A., Sanz, M.J., Arbaugh, M.J., Padgett, P.E., Jones, D.P., Davila, A., 2005. Passive sampler for monitoring ambient nitric acid (HNO_3) and nitrous acid (HNO_2) concentrations. Atmos. Environ. 39, 2655–2660.

Bytnerowicz, A., Fraczek, W., Schilling, S., Alexander, D., 2010a. Spatial and temporal distribution of ambient nitric acid and ammonia in the Athabasca Oil Sands Region, Alberta. J. Limnol. 69 (Suppl. 1), 11–21. http://dx.doi.org/10.3274/JL10-69-S1-03.

Bytnerowicz, A., Schilling, S., Alexander, D., Fraczek, W., Hansen, M., 2010b. Passive monitoring to estimate N (NO_2, HNO_3, NH_3) exposure in remote areas and geospatial analysis to optimize monitoring networks in the Athabasca Oil Sands Region. Extended Abstract 2010-A-563-AWMA. In: Proceedings of The Air and Waste Management Association 103rd Annual Conference and Exhibition, Calgary, Alberta, Canada, June 22–25, 2010.

Davies, M.J.E., 2012. Air quality modeling in the Athabasca Oil Sands Region, pp. 267–309. In: Percy, K.E. (Ed.), Developments in Environmental Science, Alberta Oil Sands: Energy, Industry and the Environment, vol. 11. Elsevier, Amsterdam.

Edmonds, R.L., Thomas, T.B., Blew, R.D., 1995. Biogeochemistry of an old-growth forested watershed, Olympic National Park, Washington. Water Resour. Bull. 31, 409–419.

Englander, J.G., Bharadwaj, S., Brandt, A.R., 2013. Historical trends in greenhouse gas emissions of the Alberta oil sands (1970–2010). Environ. Res. Lett. 8, 044036 (7 pp.).

Environment Canada, 2011. National Climate Data and Information Archive (accessed May 2014) http://climate.weather.gc.ca/.

Fenn, M.E., Poth, M.A., 2004. Monitoring nitrogen deposition in throughfall using ion exchange resin columns: a field test in the San Bernardino Mountains. J. Environ. Qual. 33, 2007–2014.

Fenn, M.E., Ross, C.S., 2010. Sulfur and nitrogen deposition monitoring in the Athabasca Oil Sands Region. Extended Abstract 2010-A-664-AWMA. In: Proceedings of The Air and Waste Management Association 103rd Annual Conference and Exhibition, Calgary, Alberta, Canada, June 22–25, 2010.

Fenn, M.E., Jovan, S., Yuan, F., Geiser, L., Meixner, T., Gimeno, B.S., 2008. Empirical and simulated critical loads for nitrogen deposition in California mixed conifer forests. Environ. Pollut. 155, 492–511.

Fenn, M.E., Sickman, J.O., Bytnerowicz, A., Clow, D.W., Molotch, N.P., Pleim, J.E., Tonnesen, G.S., Weathers, K.C., Padgett, P.E., Campbell, D.H., 2009. Methods for measuring atmospheric nitrogen deposition inputs in arid and montane ecosystems of western North America. In: Legge, A.H. (Ed.), Developments in Environmental Science, Air Quality and Ecological Impacts: Relating Sources to Effects, vol. 9. Elsevier, Amsterdam, pp. 179–228.

Fenn, M.E., Ross, C.S., Schilling, S.L., Baccus, W.D., Larrabee, M.A., Lofgren, R.A., 2013. Atmospheric deposition of nitrogen and sulfur and preferential canopy consumption of nitrate in forests of the Pacific Northwest, USA. For. Ecol. Manage. 302, 240–253.

Fields, R., 1988. Physiological responses of lichens to air pollutant fumigations. In: Nash III, T.H., Wirth, V. (Eds.), Lichens, Bryophytes and Air Quality, Bibliotheca Lichenologica, vol. 30. J. Cramer, Berlin-Stuttgart, pp. 175–200.

Flechard, C.R., Nemitz, E., Smith, R.I., Fowler, D., Vermeulen, A.T., Bleeker, A., Erisman, J.W., Simpson, D., Zhang, L., Tang, Y.S., Sutton, M.A., 2011. Dry deposition of reactive nitrogen to European ecosystems: a comparison of inferential models across the NitroEurope network. Atmos. Chem. Phys. 11, 2703–2728.

Freedman, B., Prager, U., 1986. Ambient bulk deposition, throughfall, and stemflow in a variety of forest stands in Nova Scotia. Can. J. For. Res. 16, 854–860.

Garcia-Hurtado, E., Pey, J., Borrás, E., Sánchez, P., Vera, T., Carratalá, A., Alastuey, A., Querol, X., Vallejo, V.R., 2014. Atmospheric PM and volatile organic compounds released from Mediterranean shrubland wildfires. Atmos. Environ. 89, 85–92.

Graney, J.R., Landis, M.S., Krupa, S., 2012. Coupling lead isotopes and element concentrations in epiphytic lichens to track sources of air emissions in the Athabasca oil sands region. In: Percy, K.E. (Ed.), Developments in Environmental Science, Alberta Oil Sands: Energy, Industry and the Environment, vol. 11. Elsevier, Amsterdam, pp. 343–372.

Häffner, E., Lomský, B., Hynek, V., Hällgren, J.E., Batič, F., Pfanz, H., 2001. Air pollution and lichen physiology. Physiological responses of different lichens in a transplant experiment following an SO_2-gradient. Water Air Soil Pollut. 131, 185–201.

Hazewinkel, R.R.O., Wolfe, A.P., Pla, S., Curtis, C., Hadley, K., 2008. Have atmospheric emissions from the Athabasca Oil Sands impacted lakes in northeastern Alberta, Canada? Can. J. Fish. Aquat. Sci. 65, 1554–1567.

Hecobian, A., Liu, Z., Hennigan, C.J., et al., 2011. Comparison of chemical characteristics of 495 biomass burning plumes intercepted by the NASA DC-8 aircraft during the ARCTAS/CARB-2008 field campaign. Atmos. Chem. Physic. 11, 13325–13337.

Hegg, D.A., Radke, L.F., Hobbs, P.V., Brock, C.A., Riggan, P.J., 1987. Nitrogen and sulfur emissions from the burning of forest products near large urban areas. J. Geophys. Res. 92, 14,701–14,709.

Hertel, O., Skjoth, C.A., Reis, S., Bleeker, A., Harrison, R.M., Cape, J.N., Fowler, D., Skiba, U., Simpson, D., Jickells, T., Kulmala, M., Gyldenkaerne, S., Sorensen, L.L., Erisman, J.W., Sutton, M.A., 2012. Governing processes for reactive nitrogen compounds in the European atmosphere. Biogeosciences 9, 4921–4954.

Horváth, L., 2003. Dry deposition velocity of PM2.5 ammonium sulfate particles to a Norway spruce forest on the basis of S- and N-balance estimations. Atmos. Environ. 37, 4419–4424.

Hsu, Y.-M., 2012. Ambient Air Sample Collection and Analytical Program for Integrated PM2.5, PM10, VOCs, Semi-volatile Organics, SO_2, NO_2, O_3, Wet Precipitation Chemistry, HNO_2, HNO_3, and NH_3. Report Prepared for Wood Buffalo Environmental Association, Ft. McMurray, AB, Canada, pp. 2009–2011.

Huebert, D.B., L'Hirondelle, S.J., Addison, P.A., 1985. The effects of sulphur dioxide on net CO_2 assimilation in the lichen *Evernia mesomorpha* Nyl. New Phytol. 100, 643–651.

Johnson, D.W., Lindberg, S.E., 1992. Atmospheric Deposition and Forest Nutrient Cycling: a Synthesis of the Integrated Forest Study. In: Ecol. Stud, vol. 91. Springer-Verlag, New York.

Jones, C.E., Ltd, Associates, 2007. Terrestrial Environmental Effects Monitoring: Acidification Monitoring Program. 2004 Sampling Event Report for Soils, Lichen, Understory Vegetation and Forest Health and Productivity. Prepared for:

Wood Buffalo Environmental Association, Terrestrial Environmental Effects Monitoring Committee. Fort McMurray, Alberta. 198 pp.
Jung, K., Chang, S.X., Ok, Y.S., Arshad, M.A., 2013. Critical loads and H^+ budgets of forest soils affected by air pollution from oil sands mining in Alberta, Canada. Atmos. Environ. 69, 56–64.
Klopatek, J.M., Barry, M.J., Johnson, D.W., 2006. Potential canopy interception of nitrogen in the Pacific Northwest, USA. For. Ecol. Manage. 234, 344–354.
Landis, M.S., Pancras, J.P., Graney, J.R., Stevens, R.K., Percy, K.E., Krupa, S., 2012. Receptor modeling of epiphytic lichens to elucidate the sources and spatial distribution of inorganic air pollution in the Athabasca oil sands region, pp 427–467. In: Percy, K.E. (Ed.), Developments in Environmental Science, Alberta Oil Sands: Energy, Industry and the Environment, vol. 11. Elsevier, Amsterdam.
Laxton, D.L., Watmough, S.A., Aherne, J., Straker, J., 2010. An assessment of nitrogen saturation in *Pinus banksiana* plots in the Athabasca Oil Sands Region, Alberta. J. Limnol. 69 (Suppl. 1), 171–180.
Laxton, D.L., Watmough, S.A., Aherne, J., 2012. Nitrogen cycling in *Pinus banksiana* and *Populus tremuloides* stands in the Athabasca oil sands region, Alberta, Canada. Water Air Soil Pollut. 223, 1–13.
LeBlanc, F., Rao, D.N., 1975. Effects of air pollutants on lichens and bryophytes, pp. 237–272. In: Mudd, J.B., Kozlowski, T.T. (Eds.), Response of Plants to Air Pollution. Academic Press Inc., New York.
Lovett, G.M., Lindberg, S.E., 1993. Atmospheric deposition and canopy interactions of nitrogen in forests. Can. J. For. Res. 23, 1603–1616.
McCune, B., 1988. Lichen communities along O_3 and SO_2 gradients in Indianapolis. Bryologist 91, 223–228.
Nash, T.H., Gries, C., 2002. Lichens as bioindicators of sulfur dioxide. Symbiosis 33, 1–21.
National Pollutant Release Inventory (NPRI), 2010. Environment Canada. http://www.ec.gc.ca/inrp-npri.
National Pollutant Release Inventory (NPRI), 2011. Environment Canada. http://www.ec.gc.ca/inrp-npri.
Parker, G.G., 1983. Throughfall and stemflow in the forest nutrient cycle. Adv. Ecol. Res. 13, 57–133.
Percy, K.E., Hansen, M.C., Dann, T., 2012. Air quality in the Athabasca Oil Sands Region 2011, pp. 47–91. In: Percy, K.E. (Ed.), Developments in Environmental Science, Alberta Oil Sands: Energy, Industry and the Environment, vol. 11. Elsevier, Amsterdam.
Pratt, G.C., Orr, E.J., Bock, D.C., Strassman, R.L., Fundine, D.W., Twaroski, C.J., Thornton, J.D., Meyers, T.P., 1996. Estimation of dry deposition of inorganics using filter pack data and inferred deposition velocity. Environ. Sci. Technol. 30, 2168–2177.
Proemse, B.C., Mayer, B., Fenn, M.E., 2012. Tracing industrial sulfur emissions in atmospheric sulfate deposition in the Athabasca oil sands region, Alberta, Canada. Appl. Geochem. 27, 2425–2434.
Puxbaum, H., Gregori, M., 1998. Seasonal and annual deposition rates of sulphur, nitrogen and chloride species to an oak forest in north-eastern Austria (Wolkersdorf, 240 m A.S.L.). Atmos. Environ. 32, 3557–3568.
Reid, J.S., Koppmann, R., Eck, T.F., Eleuterio, D.P., 2005. A review of biomass burning emissions part II: intensive physical properties of biomass burning particles. Atmos. Chem. Phys. 5, 799–825.
Roadman, M.J., Scudlark, J.R., Meisinger, J.J., Ullman, W.J., 2003. Validation of Ogawa passive samplers for the determinations of gaseous ammonia concentrations in agricultural settings. Atmos. Environ. 37, 2317–2325.
Root, H.T., Geiser, L.H., Fenn, M.E., Jovan, S., Hutten, M.A., Ahuja, S., Dillman, K., Schirokauer, D., Berryman, S., McMurray, J.A., 2013. A simple tool for estimating throughfall nitrogen deposition in forests of western North America using lichens. For. Ecol. Manage. 306, 1–8.
Sanz, M.J., Gries, C., Nash III, T.H., 1992. Dose-response relationships for SO_2 fumigations in the lichens *Evernia prunastri* (L.) Ach. and *Ramalina fraxinea* (L.) Ach. New Phytol. 122, 313–319.
Simkin, S.M., Lewis, D.N., Weathers, K.C., Lovett, G.M., Schwarz, K., 2004. Determination of sulfate, nitrate, and chloride in throughfall using ion-exchange resins. Water Air Soil Pollut. 153, 343–354.
Studabaker, W.B., Krupa, S., Jayanty, R.K.M., Raymer, J.H., 2012. Measurement of polynuclear aromatic hydrocarbons (PAHs) in epiphytic lichens for receptor modeling in the Athabasca oil sands region (AOSR): a pilot study, pp. 391–425. In: Percy, K.E. (Ed.), Developments in Environmental Science, Alberta Oil Sands: Energy, Industry and the Environment, vol. 11. Elsevier, Amsterdam.
Tang, H.M., Brassard, B., Brassard, R., Peake, E., 1997. A new passive sampling system for monitoring SO_2 in the atmosphere. Field Anal. Chem. Tech. 1, 307–314.
Tang, H., Lau, T., Brassard, B., Cool, W., 1999. A new all-season passive sampling system for monitoring NO_2 in air. Field Anal. Chem. Tech. 3, 338–345.
Thimonier, A., 1998. Measurement of atmospheric deposition under forest canopies: some recommendations for equipment and sampling design. Environ. Monit. Assess. 52, 353–387.
Voldner, E.C., Barrie, L.A., Sirois, A., 1986. A literature review of dry deposition of oxides of sulphur and nitrogen with emphasis on long-range transport modelling in North America. Atmos. Environ. 20, 2101–2123.
Wang, X.L., Watson, J.G., Chow, J.C., Kohl, S.D., Chen, L.-W.A., Sodeman, D.A., Legge, A.H., Percy, K.E., 2012. Measurement of real-world stack emissions with a dilution sampling system, pp. 171–192. In: Percy, K.E. (Ed.), Developments in Environmental Science, Alberta Oil Sands: Energy, Industry and the Environment, vol. 11. Elsevier, Amsterdam.
Watmough, S.A., Whitfield, C.J., Fenn, M.E., 2014. The importance of atmospheric base cation deposition for preventing soil acidification in the Athabasca Oil Sands Region of Canada. Sci. Total Environ. 493, 1–11.
Watson, J.G., Chow, J.C., Wang, X., Kohl, S.D., Gronstal, S., Zielinska, B., 2011. Winter Stack Emissions Measured with a Dilution Sampling System. Report to the Wood Buffalo Environmental Association, Ft. McMurray, Alberta, Canada. Desert Research Institute Contract Number: T113-10.
Whitfield, C.J., Aherne, J., Watmough, S.A., 2009. Modeling soil acidification in the Athabasca Oil Sands region, Alberta, Canada. Environ. Sci. Technol. 43, 5844–5850.
Wieder, R.K., Vitt, D.H., Burke-Scoll, M., Scott, K.D., House, M., Vile, M.A., 2010. Nitrogen and sulphur deposition and the growth of *Sphagnum fuscum* in bogs of the Athabasca Oil Sands Region, Alberta. J. Limnol. 69 (Suppl. 1), 161–170. http://dx.doi.org/10.3274/JL10-69-S1-16.
Zhang, L., Vet, R., O'Brien, J.M., Mihele, C., Liang, Z., Wiebe, A., 2009. Dry deposition of individual nitrogen species at eight Canadian rural sites. J. Geophys. Res. 114. D02301. 13 pp.